Molecular Biology of the Cell
Vol. 20, 4951–4961, December 1, 2009

Dcp1-Bodies in Mouse Oocytes

Adam Swetloff, Beatrice Conne, Joachim Huarte, Jean-Luc Pitetti, Serge Nef, and Jean-Dominique Vassalli

Department of Genetic Medicine and Development, Faculty of Medicine, University of Geneva, 1211 Geneva 4, Switzerland

Submitted February 12, 2009; Revised September 8, 2009; Accepted September 24, 2009
Monitoring Editor: A. Gregory Matera

Processing bodies (P-bodies) are cytoplasmic granules involved in the storage and degradation of mRNAs. In somatic cells, their formation involves miRNA-mediated mRNA silencing. Many P-body protein components are also found in germ cell granules, such as in mammalian spermatocytes. In fully grown mammalian oocytes, where changes in gene expression depend entirely on translational control, RNA granules have not as yet been characterized. Here we show the presence of P-body-like foci in mouse oocytes, as revealed by the presence of Dcp1a and the colocalization of RNA-associated protein 55 (RAP55) and the DEAD box RNA helicase Rck/p54, two proteins associated with P-bodies and translational control. These P-body-like structures have been called Dcp1-bodies and in meiotically arrested primary oocytes, two types can be distinguished based on their size. They also have different protein partners and sensitivities to the depletion of endogenous siRNA/miRNA and translational inhibitors. However, both type progressively disappear during in vitro meiotic maturation and are virtually absent in metaphase II–arrested secondary oocytes. Moreover, this disassembly of hDcp1a-bodies is concomitant with the posttranslational modification of EGFP-hDcp1a.

INTRODUCTION

Gene expression flows from DNA to protein using mRNA as an intermediate. Transcripts can either be used immediately as template for protein synthesis or translationally silenced and stored for later translation. A subset of silenced mRNAs is packaged into microscopically visible RNP granules that lack a limiting lipid membrane (Kedersha and Anderson, 2007). In mammals, processing bodies (P-bodies) RNA granules are present in a broad range of somatic cell types, including highly specialized cells such as neurons. Initially, P-bodies were discovered as 5′-3′ mRNA decay centers in mammalian somatic cells (Bashkirov *et al.,* 1997; Eystathioy *et al.,* 2003; Cougot *et al.,* 2004), and were found to be conserved in yeast (Sheth and Parker, 2003); because of the systematic localization of the decapping protein Dcp1a in P-bodies, they were also called Dcp1-bodies. Subsequently, P-bodies were shown to be involved in mRNA surveillance (Chen and Shyu, 2003; Couttet and Grange, 2004), RNA-mediated silencing (Rehwinkel *et al.,* 2005; Jakymiw *et al.,* 2005; Liu *et al.,* 2005a), and translational control (Pillai *et al.,* 2005; Liu *et al.,* 2005b; Bhattacharyya *et al.,* 2006b).

A role for P-bodies in translational control was first highlighted in yeast cells. It was shown that the entry of an mRNA into P-bodies does not automatically lead to its degradation: upon glucose starvation mRNAs can be temporarily stored in P-bodies, which increase in size and number, and then exit the foci upon refeeding to reenter polysomes (Brengues *et al.,* 2005). In mammals, this reversibility of mRNA localization has been observed for miRNA-mediated mRNA repression in Huh7 cells (Pillai, 2005; Pillai *et al.,* 2005; Bhattacharyya *et al.,* 2006a). Although such a shuttling of mRNAs between polysomes and P-bodies has not been described for other mechanisms of translational regulation, many proteins associated with translational regulation localize in P-bodies, such as 4E-T, CPEB-1, Rck-p54, and RAP55 (Andrei *et al.,* 2005; Wilczynska *et al.,* 2005; Yang *et al.,* 2006; Serman *et al.,* 2007).

Hence, in cells which rely on translational control to regulate gene expression, P-bodies or other specialized RNA granules would be expected to be present and play a role in mRNA storage. In early metazoans, the presence of germinal RNA granules has been well documented (Anderson and Kedersha, 2006); they are involved in the timing and localization of mRNA translation to promote germ cell development. *Xenopus laevis* oocytes also contain RNA granules that share protein components with somatic processing bodies and that are distinct from germinal granules (Tanaka *et al.,* 2006; Minshall *et al.,* 2007). Recently, P-body–related granules were identified in *Caenorhabditis elegans* and *Drosophila melanogaster* oocytes (Boag *et al.,* 2008; Lin *et al.,* 2008; Noble *et al.,* 2008). In mammals, specialized RNA granules called chromatoid bodies have been described in spermatocytes where translational mechanisms regulate protamine-1,2 gene expression (Kotaja *et al.,* 2006). Surprisingly, in mammalian oocytes where translational control is essential for meiotic maturation and early development, the presence of RNA-granules or P-bodies has not, to our knowledge, been reported.

In mammals, in contrast to early Metazoans, oocytes have a protracted prophase I, also known as the germinal vesicle (GV) phase, in which they remain arrested until LH (luteinizing hormone) surges stimulate the resumption of meiosis. Before prophase I arrest, transcription is shut off so that oocytes rely solely on maternal mRNA stores to complete meiosis and sustain the first cleavage divisions of the early embryo. The timely and selective expression of different transcripts, which is mediated by different translational con-

This article was published online ahead of print in *MBC in Press* (http://www.molbiolcell.org/cgi/doi/10.1091/mbc.E09–02–0123) on October 7, 2009.

Address correspondence to: Jean-Dominique Vassalli (jean-dominique.vassalli@unige.ch).

trol mechanisms, is thus crucial to mammalian gametogenesis and early development. In mouse oocytes, de novo protein synthesis is not required for resumption of meiosis (Schultz and Wassarman, 1977; Rime *et al.*, 1989), but it is essential for meiotic progression to metaphase II (MII) and extrusion of the first polar body (Clarke and Masui, 1983; Hampl and Eppig, 1995). One widely used evolutionarily conserved mechanism to activate the translation of dormant mRNAs relies on cytoplasmic polyadenylation of silenced transcripts (Hake and Richter, 1994; Sheets *et al.*, 1995; Tay *et al.*, 2000; Tay and Richter, 2001). The principal actor that mediates this process is the cytoplasmic polyadenylation element–binding protein (CPEB-1), an RNA-binding protein that, according to its state of phosphorylation, maintains maternal mRNAs in a translationally repressed state in GV oocytes and activates their translation after resumption of meiosis (Stebbins-Boaz *et al.*, 1996; Stutz *et al.*, 1997, 1998; Mendez and Richter, 2001).

Proteins with an established role in translational control in oocytes, such as CPEB-1, Rck/p54, and 4E-T have been shown to localize to P-bodies in somatic cells (Andrei *et al.*, 2005; Wilczynska *et al.*, 2005; Ferraiuolo *et al.*, 2005; Chu and Rana, 2006). In *Xenopus* oocytes, mRNA pulldown experiments have revealed that CPEB-1 specifically interacts with a number of P-body protein components, such as Rck/p54, Pat1, RAP55B, 4E-T, and an EIF4Eb protein (Minshall *et al.*, 2007), and RAP55 was found to be localized to cytoplasmic foci (Tanaka *et al.*, 2006). In the mouse, RAP55, Rck/p54, and CPEB-1 are also expressed in oocytes, but whether these protein indeed interact or form visible P-body-like foci has not been determined (Matsumoto *et al.*, 2005; Racki and Richter, 2006; Pepling *et al.*, 2007).

Recently, small noncoding RNAs (miRNAs, endogenous siRNAs, and piRNAs) were also identified in mouse oocytes (Watanabe *et al.*, 2008; Tam *et al.*, 2008). Because the link between P-bodies and RNA interference (RNAi) silencing has been well documented in somatic cells (Pillai *et al.*, 2005; Sen and Blau, 2005; Jakymiw *et al.*, 2005; Liu *et al.*, 2005b), this further suggested that mouse oocytes may also have similar RNA granules. Indeed, in somatic cells, exogenous siRNAs and miRNAs, along with the Argonautes proteins (Ago-1 and -2), which are part of the RNA-induced silencing complex (RISC), have been found particularly enriched in P-bodies (Liu *et al.*, 2005b), and depleting proteins responsible for the biogenesis of RNAi, such as Dicer or Drosha, dramatically decreased the formation of visible P-bodies (Pauley *et al.*, 2006; Eulalio *et al.*, 2007).

We therefore investigated if RNA granules are present in fully grown mouse oocytes and how they behave during meiotic maturation. We chose to study the localization of the mRNA decapping protein, Dcp1a, because this protein is a core component of many types of RNA granules: it is found in germ cell granules as well as in P-bodies. We then assessed if Rck/p54, RAP55 and CPEB colocalize with Dcp1a. Finally we tested for the presence of Dcp1a-positive foci in oocytes treated with the translational inhibitor cycloheximide, which is known to cause the dissolution of P-bodies, or depleted for small RNAs using a conditional knockout mouse for dicer.

MATERIALS AND METHODS

Oocyte Collection, Injection, and Culture

Procedures for oocyte collection from Swiss albino mice, injection, and culture have been described previously (Huarte *et al.*, 1985; Huarte *et al.*, 1987; Strickland *et al.*, 1988). For injection, fully grown oocytes were incubated in DMEM containing 5% fetal calf serum, 25 μg/ml sodium pyruvate, and 2.5 mg/ml polyvinylpyrrolidone (PVP, Amersham Pharmacia Biotech, Piscataway, NJ); a volume of ~10 pl was injected in the cytoplasm of the oocytes. Fully grown oocytes were cultured either in the presence of dB-cAMP (100 μg/μl), to prevent resumption of meiosis, or in its absence to allow meiotic maturation.

Plasmid Constructs and In Vitro Transcription

The pBS-hdcp1a-GFP plasmid was prepared by cloning the EGFP-hdcp1a fragment from C2-EGFP-hdcp1a (kind gift of Erwin van Dijk, Radboud University, Nijmegen, The Netherlands), into a pBSII-SK; the plasmid was subsequently linearized with ClaI before T7 RNA polymerase transcription (Ambion, Rotkreuz, Switzerland). The enhanced green fluorescent protein (EGFP)-dcp1a-*HA* construct was cloned by PCR amplification using the C2-EGFP-dcp1a plasmid as template with the forward primer kozak-EGFP (GGA TCC CCG GTC GCC ACC ATG GTG AGC) and the reverse primer hdcp1-hemagglutinin (HA; TCA AGC GTA ATC TGG AAC ATC GTA TGG GTA TCA TAG GTT GTG GTT GTC); the PCR product was then cloned using the TOPO-pCDNA-V5-His vector (Invitrogen, Gaithersburg, MD). Mutagenesis of pCDNA-EGFP-hdcp1a was performed following Barettino *et al.* (1994) and using the kozak-EGFP primer HA (AGC GTA ATC TGG AAC ATC GTA TGG GTA) and the F-dcp1a-495 (AGC AGA GCC CAG GAT GAG TAT). All in vitro transcriptions were performed using the Ambion T7 mMessage Machine kit (Austin, TX), and the transcripts were polyadenylated with the Ambion Poly(A) Tailing Kit (Applied Biosystems, Rotkreuz, Switzerland) as indicated by the manufacturer. All transcripts were purified by LiCl precipitation and resuspended in 150 mM KCl before injection.

Immunocytochemistry

The following primary antibodies were used: rabbit anti-hDcp1a (kind gift from J. Lykke-Andersen, University of Colorado, Boulder, CO) at 1:100, human anti-RAP55 (kind gift from D. B. Bloch, Massachusetts General Hospital and Harvard Medical School, Boston, MA) 1:200, rabbit anti-Rck/p54 (MBL, Nagoya, Japan) 1:100, rabbit anti-CPEB-1 (kind gift by J. Richter, University of Massachusetts Medical School, Worcester, MA), goat anti-CPEB N-20 (Santa Cruz Biotechnology, Santa Cruz, CA). The following secondary antibodies were used: anti-rabbit-cy3, anti-human-FITC, anti-human TRITC, anti-mouse cy3, and anti-goat cy3 (all from Jackson ImmunoResearch, West Grove, PA). All images were taken using an LSM510 Meta (Carl Zeiss AG, Jena, Germany) under a Plan Apochromat 63× 1.4 Oil DIC lens, or for live imaging using an Achroplan 63× 0.95 W lens.

Oocytes at the indicated maturation stage were fixed in 1% paraformaldehyde in M2 medium (Sigma-Aldrich, St. Louis, MO) containing 0.1% Triton X-100 for 45 min at 37°C. After three washes in PBS, 15 min each, the fixed oocytes were incubated with primary antibody overnight at 4°C. Oocytes were then washed three times in PBS, 30 min each, and incubated with secondary antibody.

Quantitative Real-Time PCR

Injected or noninjected oocytes (~100 oocytes) in GV or MII stage were lysed in 60 μl lysis buffer (20 mM Tris, pH 7.5, 5 mM Mg acetate, 100 mM NH_4Cl, 5 mM DTT, 1% NP40, 0.5% deoxycholate, 100 U/ml RNAsin, and 500 U/ml RNA guard). The lysates were extracted in 0.5 ml Trizol reagent, as described by the manufacturer (Invitrogen).

Sybr Green Real-Time PCR. The resulting RNA was reverse transcribed into cDNA using the Qiagen Sensiscript Reverse transcriptase (Qiagen, Chatsworth, CA) in a volume of 20 μl using random N15 oligonucleotides (Microsynth, Balgach, Switzerland). Real-time SYBR green PCR was performed using the Corbett rotor gene 6000 (Corbett Research UK, Cambridge, Cambridgeshire, United Kingdom) as described by the manufacturer, in a reaction volume of 10 μl using the SYBR green PCR reaction mix (Sigma-Aldrich). For each PCR reaction, a 2-μl volume of cDNA equivalent to two oocytes was used. All PCRs were performed in triplicate. Quantification was normalized to endogenous GAPDH and β-actin within the log-linear phase of the amplification curve obtained for each primer set. The data were analyzed using the comparative Ct method (Schmittgen and Livak, 2008). The primers were designed with the Roche ProbeFinder Version: 2.43 (Roche Applied Science, Indianapolis, IN; online resource at www.roche-applied-science.com/), in order to have an annealing temperature of 60°C. The primers were as follows: forward dcp1a: 5′ TGTACACTTTCTGCCCCAAA 3′; reverse dcp1a: 5′ CGGTATACAAATAACGTCCCTTCT 3′; forward EGFP: 5′ GAAGCGCGATCACATGGT 3′; reverse EGFP: 5′ CCATGCCGAGAGTGATCC 3′. forward GAPDH: 5′ TCCATGACAACTTTGGCATTG 3′; reverse GAPDH: 5′ CAGTCTTCTGGGTGGCAGTGA 3′; and forward β-actin: 5′ AAGGCCAACCGTGAAAAGAT 3′; reverse β-actin: 5′ GTGGTACGACCAGAGGCATAC 3′. The cycling program consisted of an initial step of 50°C for 2 min and 95°C for 10 min, then 40 amplification cycles of denaturation at 95°C for 15 s, and then annealing and extension at 60°C for 60 s. To evaluate the efficiency of the amplification for each primer set, a standard curve was constructed using the threshold cycle (C_T) versus 10-fold dilutions (10^{-3} to 10^{-7}) of dcp1-EGFP-transfected 293T cells.

Taqman miRNA PCR. After Trizol extraction, the RNA from isolated oocytes was reverse-transcribed and amplified with specific miRNA primers using

the Taqman miRNA assay kit (Applied Biosystems), as described by the manufacturer. PCR products were detected with the ABI PRISM SDS 7900 HT (Applied Biosystems). The miRNA expression levels for miR103, let16, and miR16 were normalized to GAPDH and β-actin using the comparative C_T method.

Western Blot

Oocytes microinjected with EGFP-dcp1a-HA mRNA either in GV or MII maturation stage were lysed in lysis buffer (20 mM Tris-HCl, pH 7.4, 150 mM NaCl, 1 mM EDTA, 1 mM EGTA, 1% [vol/vol] Triton X-100, 1× protease inhibitor mix [Roche, Switzerland], and 50 mM 2-β-mercaptoethanol) with and without potato acid phosphatase (Sigma, Poole, Dorset, United Kingdom). For oocytes not treated with phosphatase, the lysis buffer was supplemented with 1 mM Na orthovanadate and 10 mM NaF. Lysates were then lysed with 2× loading buffer (Laemmli, 1970) and boiled 3–5 min at 100°C. Of this lysate, the equivalent of 10 oocytes was loaded per lane on a 7% SDS-PAGE gel; an LMW reference ladder (Amersham, United Kingdom) was systematically added. After protein electrophoretic separation the gel was blotted on a PVDF membrane using a Mini Transblot electrophoretic transfer cell (Bio-Rad Laboratories AG, Reinach BL, Switzerland), and the blotted protein systematically revealed by Coomassie blue staining. The Western blot membrane was blocked in 5% nonfat dried milk powder (Applichem, Darmstadt, Germany) in TBS (0.1% Tween/PBS) for 1 h and incubated with primary antibody overnight at 4°C in 1% TBS, 0.1% Triton X-100, and 3% BSA. The mouse anti-HA antibody was diluted 1:1000 (Covance, Meyrin, Switzerland), the rabbit anti-tubulin 1:500, the rabbit anti-ZP3 1:1000 (Santa Cruz). The membrane was washed three times with wash buffer (1% TBS, 0.1% Triton X-100), 30 min for each wash, and incubated with secondary antibody diluted in 1% TBS, 0.1% Triton X-100, and 0.1% BSA for 2 h at room temperature. The goat anti-rabbit-HRP was diluted 1:20,000, and the anti-mouse-HRP was diluted 1:500. The membrane was then washed three times with wash buffer, 30 min for each wash, rinsed once in PBS, and sealed in a plastic wrap with ECL (Amersham), and the chemiluminescence signal was viewed by using an x-ray film.

Transgenic Mice

Dcr^{flox} (*Dcr*^{fx}) and *Gdf9Cre* mice were kindly provided by B. Harfe (University of Florida College of Medicine, Gainesville, FL) and A. J. Cooney (Baylor College of Medicine, Houston, TX), respectively, and were genotyped as described in Harfe *et al.* (2005), Lecureuil *et al.* (2002), and Lan *et al.* (2004). To achieve selective inactivation of *Dcr* in oocytes, we intercrossed transgenic *Gdf9Cre* mice expressing Cre recombinase under the control of the *Gdf9* gene promoter with mice carrying two floxed *Dcr* alleles in order to generate *Dcr*$^{fx/fx}$*;Gfd9Cre* mice lacking *Dcr* in primordial/primary oocytes. The genetic background of these mice is a mixed C57BL/6J and SV129. Genotyping for successful cre-recombination and deletion of the RNAseIII domain was done by PCR using the primers described in Harfe *et al.* (2005). *Dcr*$^{fx/fx}$*;Gfd9Cre; R26R* mice were obtained by mating the *Dcr*$^{fx/fx}$*;Gfd9Cre* mouse with a transgenic mouse bearing the open reading frame for the β-galactosidase under the ROSA26 promoter (Soriano, 1999).

Statistical Analysis

All statistics were done using the SPSS software (Chicago, IL). Independent Student's *t* test and p-ANOVA was used for comparing results between different groups. Quantification of the number of EGFP-hDcp1a foci or endogenous Dcp1a foci in confocal sections of oocytes was done using a program designed with Metamorph (Visitron, Pucheim, Germany). The software allowed detecting and discriminating small from large foci according to their size and intensity compared with background signal (courtesy of S. Starchick, University of Geneva, Geneva, Switzerland). A minimum of four confocal planes spanning each oocyte with a fixed interval was taken; the area of the oocyte in each plane was also measured using Metamorph.

RESULTS

Injection of EGFP-hdcp1a mRNA Reveals P-Body-like Structures

To investigate the presence of RNA granules in fully grown GV oocytes, we studied the expression and localization of the mRNA-decapping protein, Dcp1a, associated with both somatic P-bodies and germ cell granules. An initial RT-PCR analysis revealed that the transcript for dcp1a was present in mouse GV oocytes (Supplementary Figure S1). Because dcp1a is highly conserved in mouse and human (87% homology for the coding sequence), we chose to overexpress the cDNA sequence of human Dcp1a (hDcp1a) as an EGFP fusion protein (EGFP-hDcp1a) in live mouse GV oocytes (Figure 1). It was reasoned that this overexpression strategy would allow us to assess the dynamic localization of Dcp1a protein in real time and in live oocytes, as well as to circumvent fixation artifacts that may occur in immunocytochemical procedures. Because the transgene was of human origin,

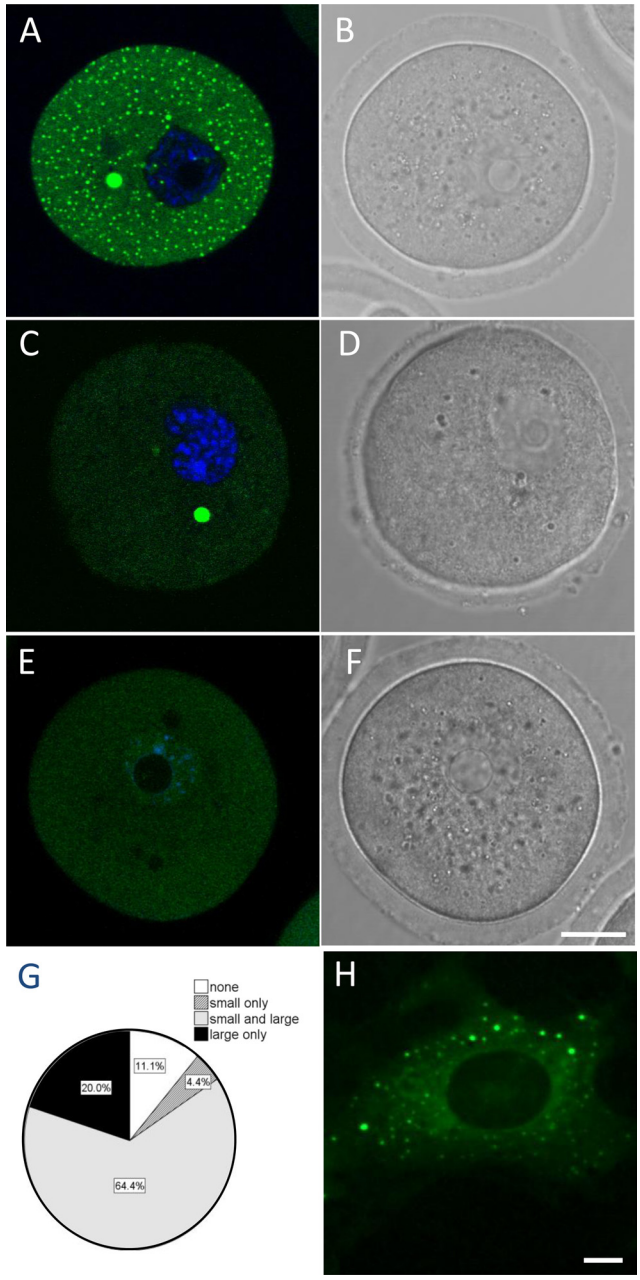

Figure 1. Overexpressed EGFP-hdcp1a forms P-body-like foci in GV oocytes. Confocal fluorescence image of oocytes in GV stage microinjected with EGFP-hdcp1a (A–D) or EGFP- (E and F) transcript. (A) A GV oocyte with both small (1–2 μm) and large (5–10 μm, arrow) EGFP-hDpc1a positive foci. (B) Equivalent bright-field image of the GV oocyte shown in A. (C) GV oocyte with only large EGFP-hDcp1a foci. (D) Equivalent bright-field image. (E) GV oocyte injected with EGFP transcript alone. (F) Equivalent bright-field image. (G) Pie chart representing the proportion of EGFP-hDcp1a-injected GV oocytes (n = 95) with no foci (11.4%), only small foci (4.4%), small and large (64.4%), and only large foci (20%). (H) Fluorescence image of an NIH3T3 cell transfected with the EGFP-hdcp1a plasmid construct. Scale bars, (A–F and H) 20 and 5 μm, respectively.

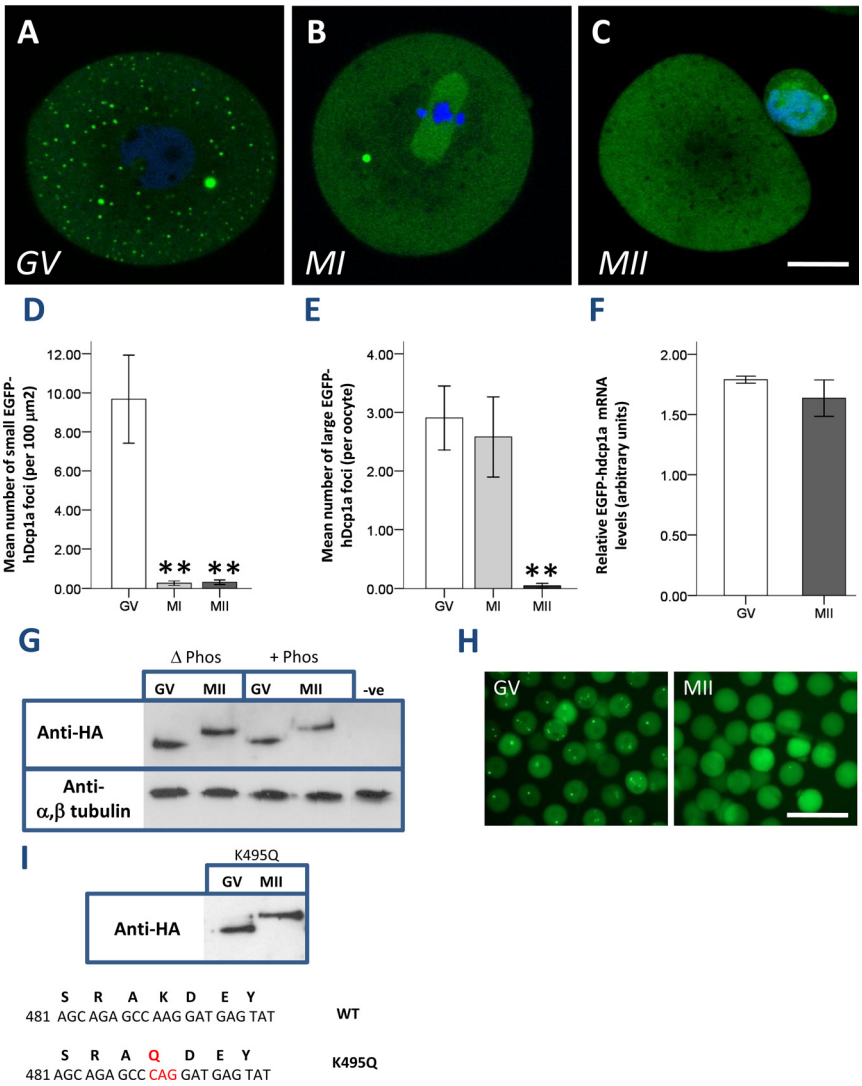

Figure 2. EGFP-hDcp1a foci disappear during oocyte meiotic maturation. Oocytes in GV stage microinjected with EGFP-hdcp1a transcript were left to mature in MI (5 h) and MII (16 h). Confocal fluorescence images of a representative: (A) GV oocyte, small and large EGFP-hDcp1a foci are seen; (B) MI oocyte, small foci have disappeared whereas large foci are still present. (C) MII oocyte, small foci remain absent and large foci have almost completely disappeared. (D) Graph showing in GV (n = 129), MI (n = 55), and MII (n = 115) the mean number of small foci (per 100 μm^2); the reduction in small foci is significant (pANOVA = 8.04×10^{-6}); (E) the mean number of large EGFP-hDcp1a foci per oocytes in GV; in MI the reduction is nonsignificant ($p = 0.89$) but significant in MII ($p = 1 \times 10^{-4}$). (F) Graph showing the relative level of EGFP-hdcp1a mRNA in GV and MII oocytes as analyzed by real-time PCR; results are normalized against GAPDH and β-actin. The percentage difference between GV and MII is 8.8% ($p = 0.153$). (G) Western blot probing for the HA-tag and α,β-tubulin on lysates of EGFP-hdcp1a-HA injected GV (n = 40) and MII oocytes (n = 40), treated with (+phos) and without (Δ phos) phosphatase, or noninjected GV oocytes (NEG). An ~11-kDa band shift of the EGFP-hDcp1a protein is seen between GV and MII stage oocytes, which is not sensitive to phosphatase treatment. (H) Fluorescence micrographs of oocytes injected with EGFP-hdcp1a mRNA in GV and MII maturation stage. (I) Western blot on lysates of GV and MII oocytes injected with EGFP-hdcp1a mRNA mutated at nucleotide 495 (K495G) and probed for the HA-tag; a band shift is still observed between GV and MII. The sequences of the predicted SUMO WT site and mutated K495G site are shown beneath. Scale bars, (A–C) 20 μm.

we first confirmed that it formed P-bodies when transfected in a mouse fibroblast cell line (NIH3T3) using a human epithelial cell line (HEK293) as control (Figure 1H).

The transcript encoding the EGFP-hDcp1a fusion protein (0.5 $\mu g/\mu l$) was microinjected in GV oocytes at a copy number (5×10^5) that was similar to the average copy number ($2–4 \times 10^5$) for transcripts present in mouse oocyte (Shim *et al.*, 1997; Steuerwald *et al.*, 2000). After 6 h, distinct fluorescent foci were clearly visible by confocal microscopy. Strikingly, of n = 95 injected oocytes analyzed from six different experiments, the majority (64.4%) bore two distinct populations of foci: small foci with a mean diameter of 0.23 μm (SD = 0.16 μm) and large foci with a mean diameter of 6.4 μm (SD = 1.2 μm; Figure 1, A–C and G). A small proportion of oocytes (20%) had only large foci and no visible small foci (Figure 1, C and D and G), whereas a lower proportion had only small granules (4.4%). Some oocytes had no visible foci (11.1%), perhaps because of suboptimal injection of the transcript. In contrast, upon microinjection of mRNA encoding EGFP alone, the protein remained diffuse in the cytoplasm (Figure 1, E and F).

Dynamic Features of EGFP-hDcp1a Foci

EGFP-hDcp1a foci were followed in time-lapse movies of oocytes undergoing maturation from GV to MI (Δt = 10 min, 3-μm sections through the whole oocyte). 3D reconstructions (n = 3, using the IMARIS software; Bitplane, Zurich, Switzerland) revealed the large foci to be dynamic structures located close to the nucleus in GV oocytes and to move away upon nuclear breakdown. The movement of the foci and their possible association to the spindle suggested similarities with microtubule-organizing centers (MTOCs; Supplementary Figure S2A); however, we did not observe any colocalization of EGFP-Dcp1a foci with an MTOCs marker (γ-tubulin), or with the microtubule protein β-tubulin (Supplementary Figure S2B).

We next investigated the behavior of EGFP-hDcp1a foci during the course of meiotic maturation. We determined the number of small and large foci in GV oocytes (n = 129), metaphase I (MI) oocytes (after 6 h of maturation, n = 55), and metaphase II (MII) oocytes (after 16 h of maturation, n = 115). We observed a dramatic reduction in the mean number (per 100 μm^2) of small foci in MI and MII oocytes (Figure 2, A–C and D). The number of large foci remained stable in MI compared with GV oocytes, whereas it was dramatically reduced in MII oocytes (Figure 2, A–C and E). Similar results were obtained in eight independent experiments.

The marked reduction of EGFP-hDcp1a foci during meiotic maturation prompted us to assess the stability of the

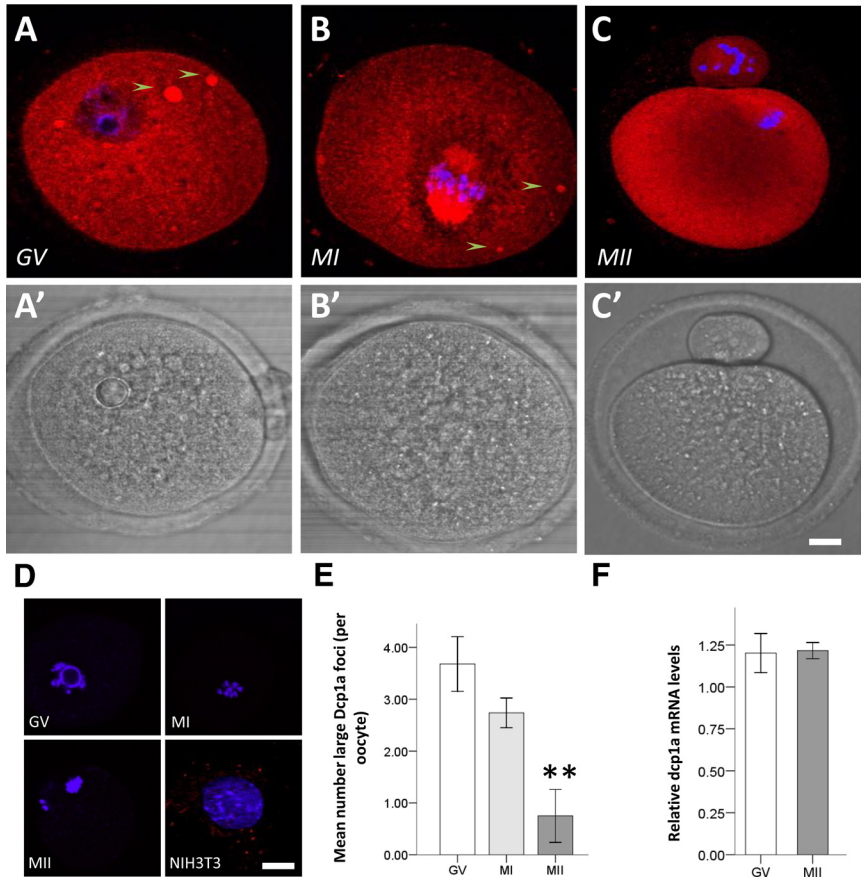

Figure 3. Endogenous Dcp1a expression during oocyte meiotic maturation. Confocal fluorescence images showing the localization of Dcp1a protein as analyzed by immunocytochemistry in a representative: (A) GV oocyte; Dcp1a is diffused in the cytoplasm and in large foci (5–10 μm), see arrows. (B) MI oocyte; staining for Dcp1a is cytoplasmic as well as strongly present on the chromosome spindle, and large Dcp1a foci are still present. (C) MII oocyte; staining for Dcp1a is present in the cytoplasm, but large Dcp1a foci are absent. (A′–C′) Bright-field images for A–C images, respectively. (D) Positive and negative controls: GV, MI, and MII oocytes showing the absence of signal when the primary antibody is omitted; a mouse NIH3T3 cell line immunostained for Dcp1a showing distinct P-body-like foci. (E) Graph showing the mean number of large Dcp1a foci in GV (n = 38), MI (n = 38), and MII (n = 22); the reduction in MI is not significant ($p = 0.098$) but is significant in MII ($p = 2 \times 10^{-3}$). (F) Graph showing the relative level of dcp1a mRNA in GV and MII oocytes as analyzed by real-time PCR and normalized against GAPDH and β-actin; no significant difference was observed ($p = 0.92$). Scale bars, (A–G) 20 μm.

injected EGFP-hDcp1a transcript. Real-time PCR, using primers designed to recognize the EGFP moiety, indicated that transcript levels were not significantly different in MII compared with GV oocytes (an 8.8% decrease, $p = 0.153$). This finding was corroborated by the fact that EGFP-hDcp1a protein was still strongly expressed, yet diffusely distributed, in MII oocytes (Figure 2F). A Western blot analysis confirmed that EGFP-hDcp1a protein was present at comparable levels in extracts of GV and MII oocytes (Figure 2G). Most strikingly, the EGFP-hDcp1a protein band shifted of ~11 kDa between GV and MII oocytes. However, this band shift was not sensitive to phosphatase treatment (Figure 2, G and H); although the activity of the phosphatase was confirmed by probing the dephosphorylation of α-phospho MAPK (mitogen-activated protein kinase) in AML12 cells treated with insulin (Supplementary Figure S3). We thus investigated if EGFP-hDcp1a was being sumoylated by small ubiquitin-like modifiers (SUMO) proteins, which are 10–12-kDa proteins that covalently bind to lysine residues of target proteins (Wilson and Rosas-Acosta, 2005). In fact, a bioinformatic analysis of hDcp1a with the Sumoylation Sites Prediction v.2.0 software (http://sumosp.biocuckoo.org/) retrieved one sumoylation site at nucleotide position 495, but mutagenesis of the critical lysine residue into a glutamine (K495G) had no effect on the band shift and dissociation of EGFP-hDcp1a foci in MII (Figure 2I). Hence, EGFP-hDcp1a foci were found to be dynamic during meiotic maturation and their disassembly in MII was not due to the degradation of the transgene but associated with the covalent posttranslational modification of hDcp1a that is neither phosphorylation nor sumoylation.

Endogenous Dcp1a Localizes to Large Foci, But Does Not Form Visible Small Foci

The localization of endogenous Dcp1a protein was explored by immunocytochemistry, using a polyclonal antibody raised against human Dcp1a. In both human 293T and mouse NIH3T3 cells Dcp1a foci were clearly visible (Figure 3). In GV oocytes, endogenous Dcp1a was diffusedly localized in the cytoplasm but also conspicuously enriched in large foci. In fact, 85% (n = 50) of oocytes bore large foci, and these had an average diameter size similar to the large foci observed upon over expression of EGFP-hDcp1a (5.90 ± 0.38 vs. 4.05 ± 0.188 μm, respectively; mean ± SE), as well as a similar frequency (3.67 ± 0.52 foci per oocyte compared with 2.90 ± 0.64, respectively). However, no small granules were apparent apart from the granular aspect of the cytoplasmic staining (Figure 3, A and A′). In MI oocytes, large Dcp1a foci were still present. In MII oocytes, they had mostly disappeared; the granular cytoplasmic staining observed in GV oocytes was also noticeably absent (Figure 3, B and C, and B′ and C′). This reduction in large Dcp1a foci (Figure 3E) mirrored that observed for the EGFP-hDcp1a foci in the overexpression study. Quantitative real-time PCR indicated that the transcript for endogenous dcp1a had not significantly decreased in MII compared with GV oocytes ($p = 0.92$; Figure 3F).

Hence, we could reveal large Dcp1a-foci by immunocytochemistry that also disappeared in MII as observed upon overexpression of EGFP-hDcp1a and independently of transcript degradation. However, small dcp1a-foci were not de-

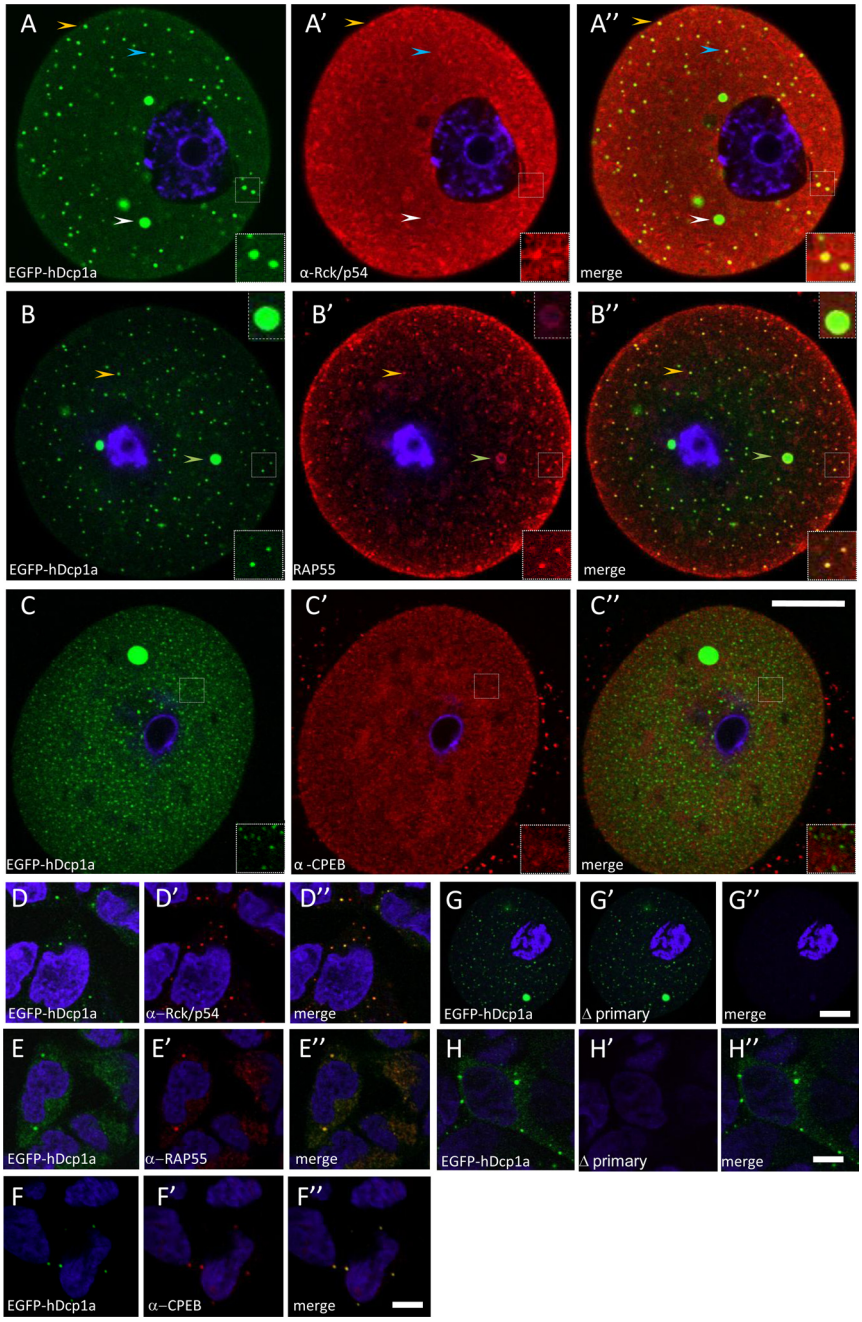

Figure 4. Colocalization of P-body markers with EGFP-hDcp1a foci in oocytes. Confocal fluorescence images of GV oocytes microinjected with EGFP-hdcp1a transcript or a HEK293 cell line stably expressing the EGFP-hdcp1a transgene, stained by immunocytochemistry for Rck/p54 (A–A″ and D–D″), RAP55 (B–B″ and E–E″), and CPEB-1 (C–C″ and F–F″). (A and D) EGFP-hDcp1a (green) expression only; A′ and D′) Rck-p54 expression (red); A″ and D″) colocalization of Rck/p54 expression with EGFP-hDcp1a (yellow). In GV oocytes, the orange arrow shows an example of small EGFP-hDpc1a foci colocalizing with Rck/p54; an inset also shows a higher magnification of small foci that have colocalized; the white arrow shows absence of colocalization with large EGFP-hDcp1a foci and the blue arrow shows absence of colocalization with small foci. In HEK-293 cells, Rck/p54 colocalizes perfectly with EGFP-hDcp1a foci. (B and E) RAP55 protein expression (red); B′ and E″) EGFP-hDcp1a expression only; (B″ and E″) colocalization of RAP55 expression with EGFP-hDcp1a (yellow); the orange arrow points at small EGFP-hDpc1a foci colocalizing with RAP55, a small dashed high magnification inset also shows small EGFP-hDcp1a foci that colocalize; the white arrow points at a colocalization with large foci (higher magnification inset also shown). In HEK-293 cells, RAP55 colocalizes with EGFP-hDcp1a foci. (C and F) CPEB-1 expression (red); (C′ and F′) EGFP-Dcp1a expression only; (C″ and F″) overlay of CPEB-1 with EGFP-hDcp1a; CPEB does not colocalize with EGFP-hDcp1a. In HEK 293 cells, CPEB-1 colocalizes with EGFP-hDcp1a foci. (G) GV oocyte injected with EGFP-hDcp1a; (G′) EGFP-hDcp1a expression only GV oocyte immunostained with only anti-rabbit and anti-human secondary antibody; (G″) overlay between G and G′. (H) HEK-293 cell line stably expressing the EGFP-hdcp1a transgene; (H′) HEK-293 cell line immunostained with only anti-rabbit and anti-human secondary antibody absence; (H″) overlay of H and H′. For each picture a high 3× magnification inset of foci is shown. Scale bar, (A–C″) 20 μm (as shown in C″ and G–G″; (D–F″ and H and H′) 5 μm (as shown in F″ and G″).

tected by immunostaining for Dcp1a protein, but this may be due to a lack of sensitivity of the procedure in oocytes.

Localization of Proteins Associated with P-Bodies

To determine if the oocyte Dcp1a foci are related to somatic P-bodies, we combined microinjection of EGFP-hdcp1a mRNA in GV oocytes with immunolocalization of proteins associated with somatic P-bodies and involved in CPE-mediated translational control. Indeed, CPEB-1 and P-body protein components RAP55, Rck/p54 colocalized with EGFP fluorescence in HEK293 cells stably expressing EGFP-hdcp1a (Figure 4, D–F″). In GV oocytes injected with EGFP-dcp1a mRNA, Rck/p54 only partially colocalized with small EGFP-hDcp1a foci; only 29% (n = 20) of small EGFP-hdcp1a foci stained for Rck-p54, whereas the larger foci appeared not to be immunostained (Figure 4, A–A″). In contrast, RAP55 was associated with all foci, both small and large (Figure 4, B–B″); immunostaining was stronger in the outer layer, perhaps because of a penetration artifact. We also noted that anti-RAP55 staining of larger foci appeared as a superficial aureole; a similar pattern was observed upon immunostaining for EGFP (not shown), suggesting that these foci are compact and not amenable to permeabilization for penetration of the antibody into their core. CPEB-1 was not detected (using an antibody provided by J. Richter) in EGFP-hDcp1a foci (Figure 4, C–C″), even though CPEB-1 was present throughout the cytoplasm at the different stages of maturation, as previously observed (Groisman *et al.*, 2000, 2001). A commercial anti-CPEB-1 (Santa Cruz) antibody was also used but the same result was obtained (not shown).

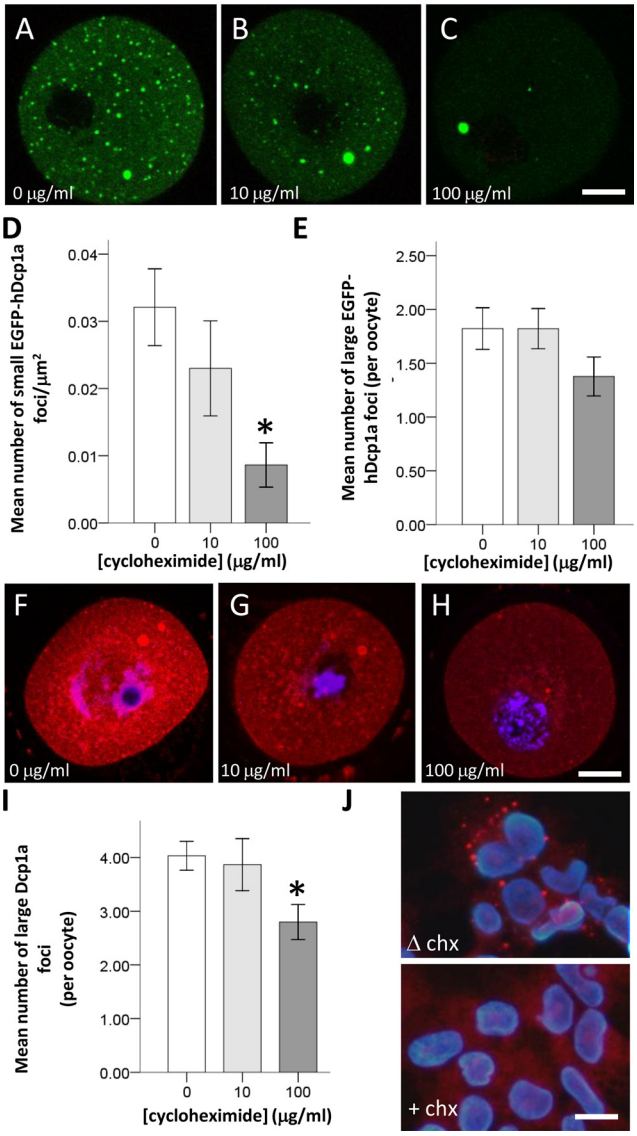

Figure 5. Only small EGFP-hDcp1a foci are sensitive to cycloheximide. (A–C) Confocal fluorescence images showing GV oocytes microinjected with EGFP-hDcp1a and treated with either 0, 10, or 100 μg/ml cycloheximide (CHX). (A) A nontreated GV oocyte showing EGFP-hDcp1a small and large foci; (B) a GV oocyte treated with 10 μg/ml CHX still showing EGFP-hDcp1a foci; (C) a GV oocyte treated with 100 μg/ml CHX. The small foci have disappeared but the large foci are still present. (D) Graph showing the mean number of small EGFP-hDcp1a foci per μm^2 for different doses of CHX; the effect of 10 μg/ml CHX (n = 56) compared with 0 μg/ml CHX (n = 45) is not significant (p = 0.45) but with 100 μg/ml CHX (n = 53) the reduction is significant ($p = 1 \times 10^{-3}$). (E) Graph showing the mean number of large EGFP-hDcp1a foci per oocyte for different doses of CHX; the effect of CHX was not significant at 10 μg/ml (p = 0.998) or at 100 μg/ml (p = 0.097). (F–H) Confocal fluorescence images of GV oocytes immunostained for Dcp1a and treated with 0 μg/ml (n = 45), 10 μg/ml (n = 50), and 100 μg/ml CHX (n = 53); large foci are present for all doses. (I) Graph showing the mean number of large Dcp1a foci per oocyte for different doses of CHX: 0 μg/ml (n = 125), 10 μg/ml (n = 30), and 100 μg/ml (n = 153), respectively; the effect of 10 μg/ml CHX was not significant (p = 0.78) but was more significant for 100 μg/ml CHX ($p = 5 \times 10^{-3}$). (J) Immunocytochemistry for Dcp1a protein in HEK-293 cells treated with (+CHX) and without (ΔCHX) cycloheximide. Scale bars, (A–C and F–H) 20 μm.

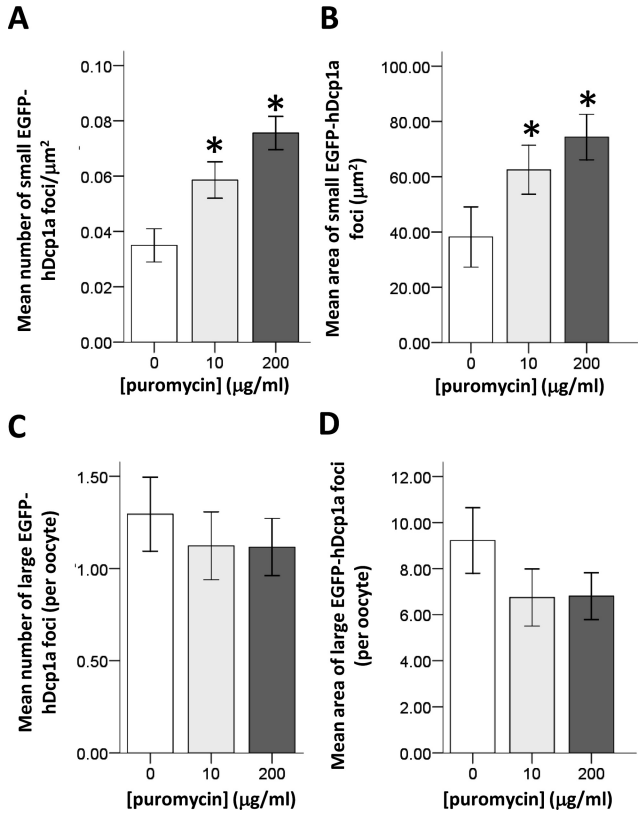

Figure 6. Puromycin increases the size and number of small EGFP-hDcp1a foci. (A) Graph showing the mean number of small EGFP-hDcp1a foci in injected GV oocytes treated with 0 μg/ml (n = 51), 10 μg/ml (n = 57), and 200 μg/ml (n = 69) puromycin; the increase is dose dependent (pANOVA = 4.7×10^{-5}). (B) Graph showing the mean size of small EGFP-hDcp1a foci in GV oocytes treated with different doses of puromycin; the increase is dose dependent (pANOVA = 0.023). (C) Graph showing the mean number per oocyte of large EGFP-hdpc1a foci in GV oocytes with 0, 10, and 200 μg/ml puromycin; the effect is nonsignificant at all doses tested ($p > 0.05$). (D) Graph showing the mean area of large EGFP-hDcp1a foci at the different doses of puromycin; the effect is nonsignificant at all doses tested ($p > 0.05$).

Inhibition of Translation by Cycloheximide and Puromycin Only Affects Small EGFP-hDcp1a Foci

In somatic cells, P-bodies disappear in presence of cycloheximide, an inhibitor or eukaryotic peptidyl transferase that freezes ribosomes on mRNA. In 293T cells treated with cycloheximide (5 μg/μl) we confirmed the total disappearance of P-bodies as revealed by immunocytochemical localization of endogenous Dcp1a (Figure 5J). We assessed the effect of a 2-h exposure to cycloheximide on the number of foci in oocytes injected and noninjected with EGFP-hdcp1a mRNA. In such GV oocytes, 10 μg/ml cycloheximide (n = 45) only marginally reduced small foci, whereas 100 μg/ml (n = 56) reduced these by 70.8%, compared with control oocytes (n = 53; p = 0.001; Figure 5, A–C and D). Large EGFP-hDdcp1a foci were not significantly affected at all doses of cycloheximide tested ($p > 0.05$; Figure 6, A–C and E). Similarly, in noninjected oocytes, the large Dcp1a-foci were only slightly affected when treated with 100 μg/ml cycloheximide (n = 153) compared with controls (n = 125; p = 0.05), and there was no significant difference in presence of 10 μg/ml cycloheximide (n = 30; $p > 0.78$; Figure 6, F–H and I).

We also addressed the effect of puromycin on EGFP-hDcp1a foci in GV oocytes. Puromycin is an aminoacyl-tRNA analog that interferes with peptidyl transfer resulting in premature termination. Contrary to cycloheximide's effect, puromycin causes the release of ribosomes and the increase in size and number of P-bodies in somatic cells (Eulalio *et al.*, 2007; Zheng *et al.*, 2008). We could show that 10 μg/ml puromycin efficiently inhibited translation as it completely inhibited maturation to metaphase II, which relies on de novo translation. We also confirmed by zymography that the translational activation of tPA that normally occurs during maturation was inhibited (not shown). We found that in oocytes injected with EGFP-hdcp1a mRNA and treated with 10 μg/ml (n = 59) and 200 μg/ml (n = 69) puromycin, the number of small EGFP-hDcp1a foci increased in a dose-dependent manner compared with control oocytes (n = 51; pANOVA = 4.7×10^{-5} and pANOVA = 0.023, respectively; Figure 6, A and B). In contrast, large hDcp1a foci were not significantly affected either in number or size at any of the puromycin concentrations ($p > 0.05$; Figure 6, C and D).

Depletion of Small RNAs Only Marginally Decreases Small EGFP-hDpc1a Foci

To determine whether the Dcp1a foci require the presence of small noncoding RNAs, such as miRNAs and endogenous siRNAs whose synthesis depends on the activity of the dicer protein (Tam *et al.*, 2008), we used a conditional knockout approach to inactivate *Dicer* (*Dcr*) specifically in oocytes. We crossed mice in which the *Dcr* gene was floxed around exon 24, encoding most of the second RNAse III domain (Figure 7A; provided by Harfe *et al.*, 2005), with transgenic mice in which the Cre-recombinase is under the control of the growth and differentiation factor-9 (gdf-9) promoter and thus exclusively expressed in oocytes of primordial and later stage follicles (Lan *et al.*, 2004). Early inactivation of dicer should lead to the total depletion of small RNAs in fully grown oocytes.

To confirm the specificity of Dicer ablation in oocytes, we crossed *Dcr$^{fx/fx}$;Gdf9Cre* with R26R-β-galactosidase reporter mice (Soriano, 1999), and show that β-galactosidase activity was exclusively located in the oocytes of primordial follicles and follicles at later developmental stages (Figure 7B). In fully grown oocytes isolated from *Dcr$^{fx/fx}$;Gdf9Cre* mice, transcription of the exon 24 of *Dcr* was indeed essentially undetectable (Figure 7C). In addition, small RNAs such as miR103, miR16, and let7a, which are abundant in wild-type mouse oocytes (Tam *et al.*, 2008), were reduced by 93.2, 85.4, and 87.3%, respectively in *Dcr$^{-/-}$* oocytes (Figure 7D). Similar to those observed in previous publications (Murchison *et al.*, 2007), *Dcr$^{-/-}$* oocytes exhibited maturation defects, in that significantly fewer matured to MI and MII oocytes compared with control oocytes (Figure 7E).

Having shown that *Dcr$^{-/-}$* oocytes were depleted of miRNAs, we investigated whether Dcp1a foci were affected. When EGFP-hDcp1a was overexpressed, the number of small foci was reduced by 40% in *Dcr$^{-/-}$* compared with control oocytes (Figure 7, F and H). In contrast, the number of large foci was not significantly altered (Figure 7, F and G). No significant difference in the number of endogenous Dcp1a large foci was observed between *Dcr$^{-/-}$* and control oocytes (Figure 7, I and J).

DISCUSSION

Two Types of Dcp1-Bodies in Mouse Oocytes

In the present study, we have revealed in isolated mouse primary oocytes the existence of two types of P-body-like granules, which could be macroscopically distinguished based on their size: the larger granules, were 5–10 μm in size and often were close to the nucleus; small foci were 0.5–2 μm in size and were more P-body-like in appearance. Both types were called Dcp1-bodies because they were revealed by over expression of an EGFP-hDcp1a fusion construct, as well as by probing for the endogenous Dcp1a protein. Although the expression of the EGFP-hDcp1a transgene revealed these two types of Dcp1-bodies, the endogenous form of Dcp1a was only apparent in the large Dcp1-bodies. Although staining of the cytoplasm for Dcp1a was granular in appearance, visible small foci were not present. This discrepancy may reflect either a technical limitation inherent to the immunocytochemistry method, because of a low sensitivity of detection or that the overexpression of Dcp1a promotes the formation of smaller foci, thus emphasizing a mechanism that is already present in oocytes. Of course, it cannot be excluded that the appearance of smaller foci is merely a result of the abnormal expression of the transgene protein. Some variation in the average number of small and large Dcp1-bodies was also observed between different sets of experiments. This could either be due to different exposures to stress when the oocytes are isolated, or in the case of injected oocytes, to the quality of the transcript used and the amount that is injected.

The Dcp1-Bodies Are Dynamic during Meiotic Maturation

Most remarkably, the Dcp1-bodies were highly dynamic during the course of meiotic maturation: small EGFP-hDcp1a bodies disappeared very quickly upon GV breakdown (GVBD) and entry into MI, whereas larger foci receded only in MII. This is reminiscent of the variation of somatic P-body formation during the cell cycle: the majority of P-bodies disassemble during mitosis and reassemble in G1 (Yang *et al.*, 2004). Moreover, because many maternal mRNAs are translationally repressed in arrested primary mouse oocytes and are later translated upon resumption of meiosis, it is striking that the presence of Dcp1-bodies mirrors this process.

Intriguingly, the disassembly of EGFP-hDcp1a foci in MII was concomitant with the covalent posttranslational modification of the EGFP-hDcp1a protein. It has been recently reported that during neural development as well as in HEK cells treated with arsenate, Dcp1a is phosphorylated (Blumenthal *et al.*, 2009). However, the posttranslational modification we observed was not sensitive to phosphatase treatment. We were also able show that the transgene was not sumoylated using a mutagenesis approach for the predicted SUMO site of hDcp1a. It is therefore possible that another yet unknown posttranslational modification is involved.

Mouse Oocyte Small Dcp1-Bodies are RNA Granules

Because the formation of P-bodies in somatic cells is known to depend on mRNA and miRNAs/siRNAs (Eulalio *et al.*, 2007), we tested whether this was also the case for small and large Dcp1-bodies in mouse oocytes. Under similar conditions in mouse oocytes, only the smaller Dcp1-bodies were affected by cycloheximide and puromycin treatments: the response to the latter being stronger. It thus appears that as shown for P-bodies, ribosome-free mRNAs are also recruited at least to smaller Dcp1-bodies.

When small RNAs that depend on Dicer for their biogenesis were depleted, smaller dcp1-bodies were only marginally reduced in number, whereas larger foci were unaffected. This may however reflect the fact that there are many Dicer-independent small noncoding RNAs that are present in the oocyte. Indeed, in another oocyte-specific conditional mouse knockout for dicer (*Dcr$^{fx/fx}$;Zp3Cre*), only 18.4% of transcripts tested was significantly changed (Murchison *et al.*, 2007). Furthermore, the

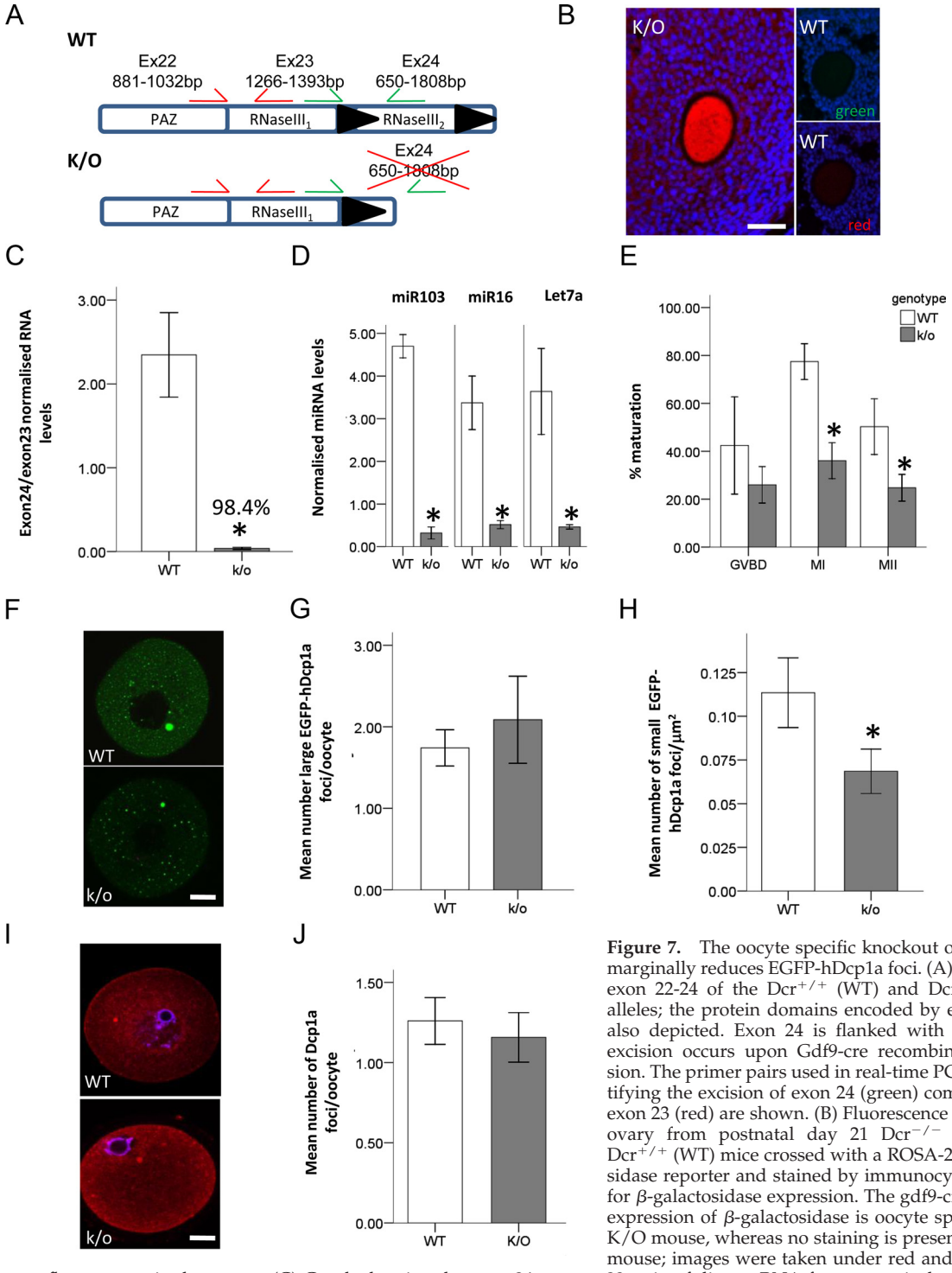

Figure 7. The oocyte specific knockout of dicer only marginally reduces EGFP-hDcp1a foci. (A) Diagram of exon 22-24 of the $Dcr^{+/+}$ (WT) and $Dcr^{-/-}$ (K/O) alleles; the protein domains encoded by each exon is also depicted. Exon 24 is flanked with lox P sites, excision occurs upon Gdf9-cre recombinase expression. The primer pairs used in real-time PCR for quantifying the excision of exon 24 (green) compared with exon 23 (red) are shown. (B) Fluorescence image of an ovary from postnatal day 21 $Dcr^{-/-}$ (K/O) and $Dcr^{+/+}$ (WT) mice crossed with a ROSA-26 β-galactosidase reporter and stained by immunocytochemistry for β-galactosidase expression. The gdf9-cre mediated expression of β-galactosidase is oocyte specific in the K/O mouse, whereas no staining is present in the WT mouse; images were taken under red and green filter showing no auto-fluorescence in the oocyte. (C) Graph showing the exon 24 to exon 23 ratio of dicer mRNA for oocytes isolated from WT (n = 3) and K/O (n = 3) mice as quantified by real-time PCR. (D) Graph showing the normalized miRNA levels in oocytes isolated from dicer WT (n = 3) and K/O (n = 3) mice. (E) Graph showing the percentage maturation of oocytes from dicer WT (n = 6) and K/O (n = 6) mice. The different stages of meiotic maturation are GV breakdown (GVBD), after 2-h maturation; MI, after 5-h maturation; and MII, after 16-h maturation. (F) Confocal fluorescence micrographs of dicer WT and K/O oocytes injected with EGFP-hdcp1a transcript. (G and H) Graph showing the quantification of the mean number of large and small EGFP-hDcp1a foci in WT (n = 178) and K/O (n = 138) oocytes, respectively. For small foci, a 40% reduction ($p = 0.04$) was observed, whereas there was no significant difference observed for large foci ($p = 0.601$). (I) Fluorescence micrograph of WT (n = 200) and K/O (n = 231) oocytes stained for Dcp1a by immunocytochemistry. (J) Graph showing the mean number of immunostained Dcp1a foci in WT and K/O oocytes. Scale bars, (F and I) 20 μm; (B) 50 μm.

mouse oocyte also harbors a specialized form of small RNAs, whose biogenesis is independent of Dicer. These piRNAs have been shown to localize to the chromatoid body in spermatocytes and recently, piRNAs have been shown to localize with a

subset of P-body-like structures present in *Drosophila* germ line cells (Lim *et al.*, 2009).

Mouse Oocyte Dcp1-Bodies Share Proteins Associated with P-Bodies

When probing for proteins that are normally associated with somatic P-bodies, it was found that large and smaller Dcp1-bodies actually colocalized with distinct protein partners. RAP55 localized to both small and large Dcp1-bodies, whereas Rck/p54 only localized to the former. This may suggest a different function for small and large Dcp1-bodies. Also, because two orthologues of RAP55 have been observed in vertebrates, namely RAP55A and RAP55B (Minshall *et al.*, 2007), it cannot be excluded that the human serum we used to detect RAP55 recognizes one form that is localizing to small Dcp1-bodies and another form that is localizing to large Dcp1-foci. In addition, the colocalization of Rck/p54 with only a subset of the smaller Dcp1-bodies suggests that there may be different subtypes of small Dcp1-bodies as observed in germ cells of early metazoans (Noble *et al.*, 2008).

The lack of interaction between Dcp1-bodies and CPEB-1 was surprising. Indeed, in GV oocytes, many mRNAs are translationally repressed by a CPEB-mediated mechanism and become activated only upon resumption of meiosis (Stutz *et al.*, 1998; Oh *et al.*, 2000). It would thus appear that mRNAs maintained as CPE-mediated repressed transcripts are stored independently of Dcp1-bodies in oocytes. This would be compatible with the observation that translational repression does not in fact depend upon P-body formation (Decker *et al.*, 2007; Eulalio *et al.*, 2007).

Dcp1-Bodies Are Reminiscent of Early Metazoan P-Body-like Germ Cell Granules

Intriguingly, the Dcp1-bodies we observe, and especially the smaller type, have similar characteristics to P-body related granules reported in oocytes of early metazoans (Noble *et al.*, 2008). In *D. melanogaster* oocytes, Dcp1 foci have also been observed but differ from somatic P-bodies in that they lack the decapping protein, Dcp2. Furthermore, these Dcp1 foci are insensitive to cycloheximide (Lin *et al.*, 2008). Similarly, in *C. elegans*, P-body related foci were also reported (Boag *et al.*, 2008; Noble *et al.*, 2008). Two populations of foci were characterized, one enriched for the decapping protein Dcp2 (dcp-bodies) and another specific for RAP55 and the Rck/p54 homologues (grp-bodies).

In *Drosophila* germ cells, it is now known that a significant proportion of P-body-like foci play a role in piRNA-mediated silencing of retro-elements (Lim *et al.*, 2009). It is therefore possible that a similar conserved mechanism is present in mouse oocytes; this would explain why Dcp1-bodies do not colocalize with CPEB and are insensitive to *dicer* deletion.

Interestingly, in *C. elegans* and *D. melanogaster*, it has been shown that somatic-like P-bodies only appear during early embryogenesis. In mouse two-cell embryos, one study colocalized dcp1a foci with argonaute-2, an RNAi-associated protein, but whether these granules are somatic P-bodies was not investigated (Lykke-Andersen *et al.*, 2008). The observation that Dcp1-bodies reappear in early embryos while we find that they disappear in MII oocytes underlines the dynamic nature of these structures. It is thus possible that Dcp1-bodies change their protein partners and thus their function during the course of meiotic maturation and early development, as described in early metazoans.

ACKNOWLEDGMENTS

We are grateful to Prof. Belin for scientific advice, as well as to the bioimaging platform at the Centre Medical Universitaire, University of Geneva (Olivier Brun, Serge Arnaudeau, Sergei Startchick) for help in the acquisition and analysis of the micrographs. We also to thank Chantal Combepine for her assistance and involvement in many of the experiments described. Last but not least, we thank Yannick Romero (University of Geneva, Geneva, Switzerland) for sharing the dicer mouse. We are indebted to the Fonds National Suisse de la Recherche Scientifique for generous funding.

REFERENCES

Anderson, P., and Kedersha, N. (2006). RNA granules. J. Cell Biol. *172*, 803–808.

Andrei, M. A., Ingelfinger, D., Heintzmann, R., Achsel, T., Rivera-Pomar, R., and Luhrmann, R. (2005). A role for eIF4E and eIF4E-transporter in targeting mRNPs to mammalian processing bodies. RNA *11*, 717–727.

Barettino, D., Feigenbutz, M., Valcarcel, R., and Stunnenberg, H. G. (1994). Improved method for PCR-mediated site-directed mutagenesis. Nucleic Acids Res. *22*, 541–542.

Bashkirov, V. I., Scherthan, H., Solinger, J. A., Buerstedde, J. M., and Heyer, W. D. (1997). A mouse cytoplasmic exoribonuclease (mXRN1p) with preference for G4 tetraplex substrates. J. Cell Biol. *136*, 761–773.

Bhattacharyya, S. N., Habermacher, R., Martine, U., Closs, E. I., and Filipowicz, W. (2006a). Relief of microRNA-mediated translational repression in human cells subjected to stress. Cell *125*, 1111–1124.

Bhattacharyya, S. N., Habermacher, R., Martine, U., Closs, E. I., and Filipowicz, W. (2006b). Stress-induced reversal of microRNA repression and mRNA P-body localization in human cells. Cold Spring Harb. Symp. Quant. Biol. *71*, 513–521.

Blumenthal, J., Behar, L., Elliott, E., and Ginzburg, I. (2009). Dcp1a phosphorylation along neuronal development and stress. FEBS Lett. *583*, 197–201.

Boag, P.R., Atalay, A., Robida, S., Reinke, V., and Blackwell, T.K. (2008). Protection of specific maternal messenger RNAs by the P body protein CGH-1 (Dhh1/RCK) during *Caenorhabditis elegans* oogenesis. J. Cell Biol. *182*, 543–557.

Brengues, M., Teixeira, D., and Parker, R. (2005). Movement of eukaryotic mRNAs between polysomes and cytoplasmic processing bodies. Science *310*, 486–489.

Chen, C. Y., and Shyu, A. B. (2003). Rapid deadenylation triggered by a nonsense codon precedes decay of the RNA body in a mammalian cytoplasmic nonsense-mediated decay pathway. Mol. Cell. Biol. *23*, 4805–4813.

Chu, C. Y., and Rana, T. M. (2006). Translation repression in human cells by microRNA-induced gene silencing requires RCK/p54. PLoS Biol. *4*, e210.

Clarke, H. J. and Masui, Y. (1983). The induction of reversible and irreversible chromosome decondensation by protein synthesis inhibition during meiotic maturation of mouse oocytes. Dev. Biol. *97*, 291–301.

Cougot, N., Babajko, S., and Seraphin, B. (2004). Cytoplasmic foci are sites of mRNA decay in human cells. J. Cell Biol. *165*, 31–40.

Couttet, P., and Grange, T. (2004). Premature termination codons enhance mRNA decapping in human cells. Nucleic Acids Res. *32*, 488–494.

Decker, C. J., Teixeira, D., and Parker, R. (2007). Edc3p and a glutamine/asparagine-rich domain of Lsm4p function in processing body assembly in *Saccharomyces cerevisiae*. J. Cell Biol. *179*, 437–449.

Eulalio, A., Behm-Ansmant, I., Schweizer, D., and Izaurralde, E. (2007). P-body formation is a consequence, not the cause, of RNA-mediated gene silencing. Mol. Cell. Biol. *27*, 3970–3981.

Eystathioy, T., Jakymiw, A., Chan, E. K., Seraphin, B., Cougot, N., and Fritzler, M. J. (2003). The GW182 protein colocalizes with mRNA degradation associated proteins hDcp1 and hLSm4 in cytoplasmic GW bodies. RNA *9*, 1171–1173.

Ferraiuolo, M. A., Basak, S., Dostie, J., Murray, E. L., Schoenberg, D. R., and Sonenberg, N. (2005). A role for the eIF4E-binding protein 4E-T in P-body formation and mRNA decay. J. Cell Biol. *170*, 913–924.

Groisman, I., Huang, Y. S., Mendez, R., Cao, Q., and Richter, J. D. (2001). Translational control of embryonic cell division by CPEB and maskin. Cold Spring Harb. Symp. Quant. Biol. *66*, 345–351.

Groisman, I., Huang, Y. S., Mendez, R., Cao, Q., Theurkauf, W., and Richter, J. D. (2000). CPEB, maskin, and cyclin B1 mRNA at the mitotic apparatus: implications for local translational control of cell division. Cell *103*, 435–447.

Hake, L. E., and Richter, J. D. (1994). CPEB is a specificity factor that mediates cytoplasmic polyadenylation during *Xenopus* oocyte maturation. Cell *79*, 617–627.

Hampl, A., and Eppig, J. J. (1995). Translational regulation of the gradual increase in histone H1 kinase activity in maturing mouse oocytes. Mol. Reprod. Dev. *40*, 9–15.

Harfe, B.D., McManus, M. T., Mansfield, J. H., Hornstein, E., and Tabin, C. J. (2005). The RNaseIII enzyme Dicer is required for morphogenesis but not patterning of the vertebrate limb. Proc. Natl. Acad. Sci. USA *102*, 10898–10903.

Huarte, J., Belin, D., Vassalli, A., Strickland, S., and Vassalli, J. D. (1987). Meiotic maturation of mouse oocytes triggers the translation and polyadenylation of dormant tissue-type plasminogen activator mRNA. Genes Dev. *1*, 1201–1211.

Huarte, J., Belin, D., and Vassalli, J. D. (1985). Plasminogen activator in mouse and rat oocytes: induction during meiotic maturation. Cell *43*, 551–558.

Jakymiw, A., Lian, S., Eystathioy, T., Li, S., Satoh, M., Hamel, J. C., Fritzler, M. J., and Chan, E. K. (2005). Disruption of GW bodies impairs mammalian RNA interference. Nat. Cell Biol. *7*, 1267–1274.

Kedersha, N. and Anderson, P. (2007). Mammalian stress granules and processing bodies. Methods Enzymol. *431*, 61–81.

Kotaja, N., Bhattacharyya, S. N., Jaskiewicz, L., Kimmins, S., Parvinen, M., Filipowicz, W., and Sassone-Corsi, P. (2006). The chromatoid body of male germ cells: similarity with processing bodies and presence of Dicer and microRNA pathway components. Proc. Natl. Acad. Sci. USA *103*, 2647–2652.

Laemmli, U. K. (1970). Cleavage of structural proteins during the assembly of the head of bacteriophage T4. Nature *227*, 680–685.

Lan, Z. J., Xu, X., and Cooney, A. J. (2004). Differential oocyte-specific expression of Cre recombinase activity in GDF-9-iCre, Zp3cre, and Msx2Cre transgenic mice. Biol. Reprod. *71*, 1469–1474.

Lecureuil, C., Fontaine, I., Crepieux, P., and Guillou, F. (2002). Sertoli and granulosa cell-specific Cre recombinase activity in transgenic mice. Genesis *33*, 114–118.

Lim, A. K., Tao, L., and Kai, T. (2009). piRNAs mediate posttranscriptional retroelement silencing and localization to pi-bodies in the *Drosophila* germline. J. Cell Biol. *186*, 333–342.

Lin, M. D., Jiao, X., Grima, D., Newbury, S. F., Kiledjian, M., and Chou, T. B. (2008). *Drosophila* processing bodies in oogenesis. Dev. Biol. *322*, 276–288.

Liu, J., Rivas, F. V., Wohlschlegel, J., Yates, J. R., III, Parker, R., and Hannon, G. J. (2005a). A role for the P-body component GW182 in microRNA function. Nat. Cell Biol. *7*, 1261–1266.

Liu, J., Valencia-Sanchez, M. A., Hannon, G. J., and Parker, R. (2005b). MicroRNA-dependent localization of targeted mRNAs to mammalian P-bodies. Nat. Cell Biol. *7*, 719–723.

Lykke-Andersen, K., Gilchrist, M. J., Grabarek, J. B., Das, P., Miska, E., and Zernicka-Goetz, M. (2008). Maternal Argonaute 2 is essential for early mouse development at the maternal-zygotic transition. Mol. Biol. Cell *19*, 4383–4392.

Matsumoto, K., Kwon, O. Y., Kim, H., and Akao, Y. (2005). Expression of rck/p54, a DEAD-box RNA helicase, in gametogenesis and early embryogenesis of mice. Dev. Dyn. *233*, 1149–1156.

Mendez, R. and Richter, J. D. (2001). Translational control by CPEB: a means to the end. Nat. Rev. Mol. Cell Biol. *2*, 521–529.

Minshall, N., Reiter, M. H., Weil, D., and Standart, N. (2007). CPEB interacts with an ovary-specific eIF4E and 4E-T in early *Xenopus* oocytes. J. Biol. Chem. *282*, 37389–37401.

Murchison, E. P., Stein, P., Xuan, Z., Pan, H., Zhang, M. Q., Schultz, R. M., and Hannon, G. J. (2007). Critical roles for Dicer in the female germline. Genes Dev. *21*, 682–693.

Noble, S. L., Allen, B. L., Goh, L. K., Nordick, K., and Evans, T. C. (2008). Maternal mRNAs are regulated by diverse P body-related mRNP granules during early *Caenorhabditis elegans* development. J. Cell Biol. *182*, 559–572.

Oh, B., Hwang, S., McLaughlin, J., Solter, D., and Knowles, B. B. (2000). Timely translation during the mouse oocyte-to-embryo transition. Development *127*, 3795–3803.

Pauley, K. M., Eystathioy, T., Jakymiw, A., Hamel, J. C., Fritzler, M. J., and Chan, E. K. (2006). Formation of GW bodies is a consequence of microRNA genesis. EMBO Rep. *7*, 904–910.

Pepling, M. E., Wilhelm, J. E., O'Hara, A. L., Gephardt, G. W., and Spradling, A. C. (2007). Mouse oocytes within germ cell cysts and primordial follicles contain a Balbiani body. Proc. Natl. Acad. Sci. USA *104*, 187–192.

Pillai, R. S. (2005). MicroRNA function: multiple mechanisms for a tiny RNA? RNA *11*, 1753–1761.

Pillai, R. S., Bhattacharyya, S. N., Artus, C. G., Zoller, T., Cougot, N., Basyuk, E., Bertrand, E., and Filipowicz, W. (2005). Inhibition of translational initiation by Let-7 MicroRNA in human cells. Science *309*, 1573–1576.

Racki, W. J. and Richter, J. D. (2006). CPEB controls oocyte growth and follicle development in the mouse. Development *133*, 4527–4537.

Rehwinkel, J., Behm-Ansmant, I., Gatfield, D., and Izaurralde, E. (2005). A crucial role for GW182 and the DCP1, DCP2 decapping complex in miRNA-mediated gene silencing. RNA *11*, 1640–1647.

Rime, H., Neant, I., Guerrier, P., and Ozon, R. (1989). 6-Dimethylaminopurine (6-DMAP), a reversible inhibitor of the transition to metaphase during the first meiotic cell division of the mouse oocyte. Dev. Biol. *133*, 169–179.

Schmittgen, T. D., and Livak, K. J. (2008). Analyzing real-time PCR data by the comparative C(T) method. Nat. Protoc. *3*, 1101–1108.

Schultz, R. M., and Wassarman, P. M. (1977). Biochemical studies of mammalian oogenesis: Protein synthesis during oocyte growth and meiotic maturation in the mouse. J. Cell Sci. *24*, 167–194.

Sen, G. L., and Blau, H. M. (2005). Argonaute 2/RISC resides in sites of mammalian mRNA decay known as cytoplasmic bodies. Nat. Cell Biol. *7*, 633–636.

Serman, A., Le, R. F., Aigueperse, C., Kress, M., Dautry, F., and Weil, D. (2007). GW body disassembly triggered by siRNAs independently of their silencing activity. Nucleic Acids Res. *35*, 4715–4727.

Sheets, M. D., Wu, M., and Wickens, M. (1995). Polyadenylation of c-mos mRNA as a control point in *Xenopus* meiotic maturation. Nature *374*, 511–516.

Sheth, U., and Parker, R. (2003). Decapping and decay of messenger RNA occur in cytoplasmic processing bodies. Science *300*, 805–808.

Shim, C., Lee, S. G., Song, W. K., Lee, C. S., Lee, K. K., and Kim, K. (1997). Laminin chain-specific gene expression during mouse oocyte maturation. Mol. Reprod. Dev. *48*, 185–193.

Soriano, P. (1999). Generalized lacZ expression with the ROSA26 Cre reporter strain. Nat. Genet. *21*, 70–71.

Stebbins-Boaz, B., Hake, L. E., and Richter, J. D. (1996). CPEB controls the cytoplasmic polyadenylation of cyclin, Cdk2 and c-mos mRNAs and is necessary for oocyte maturation in *Xenopus*. EMBO J. *15*, 2582–2592.

Steuerwald, N., Cohen, J., Herrera, R. J., and Brenner, C. A. (2000). Quantification of mRNA in single oocytes and embryos by real-time rapid cycle fluorescence monitored RT-PCR. Mol. Hum. Reprod. *6*, 448–453.

Strickland, S., Huarte, J., Belin, D., Vassalli, A., Rickles, R. J., and Vassalli, J. D. (1988). Antisense RNA directed against the 3′ noncoding region prevents dormant mRNA activation in mouse oocytes. Science *241*, 680–684.

Stutz, A., Conne, B., Huarte, J., Gubler, P., Volkel, V., Flandin, P., and Vassalli, J. D. (1998). Masking, unmasking, and regulated polyadenylation cooperate in the translational control of a dormant mRNA in mouse oocytes. Genes Dev. *12*, 2535–2548.

Stutz, A., Huarte, J., Gubler, P., Conne, B., Belin, D., and Vassalli, J. D. (1997). In vivo antisense oligodeoxynucleotide mapping reveals masked regulatory elements in an mRNA dormant in mouse oocytes. Mol. Cell. Biol. *17*, 1759–1767.

Tam, O. H. *et al*. (2008). Pseudogene-derived small interfering RNAs regulate gene expression in mouse oocytes. Nature *453*, 534–538.

Tanaka, K. J., Ogawa, K., Takagi, M., Imamoto, N., Matsumoto, K., and Tsujimoto, M. (2006). RAP55, a cytoplasmic mRNP component, represses translation in *Xenopus* oocytes. J. Biol. Chem. *281*, 40096–40106.

Tay, J., Hodgman, R., and Richter, J. D. (2000). The control of cyclin B1 mRNA translation during mouse oocyte maturation. Dev. Biol. *221*, 1–9.

Tay, J., and Richter, J. D. (2001). Germ cell differentiation and synaptonemal complex formation are disrupted in CPEB knockout mice. Dev. Cell *1*, 201–213.

Watanabe, T., Imai, H., and Minami, N. (2008). Identification and expression analysis of small RNAs during development. Methods Mol. Biol. *442*, 173–185.

Wilczynska, A., Aigueperse, C., Kress, M., Dautry, F., and Weil, D. (2005). The translational regulator CPEB1 provides a link between dcp1 bodies and stress granules. J. Cell Sci. *118*, 981–992.

Wilson, V. G. and Rosas-Acosta, G. (2005). Wrestling with SUMO in a new arena. Sci. STKE 2005, e32.

Yang, W. H., Yu, J. H., Gulick, T., Bloch, K. D., and Bloch, D. B. (2006). RNA-associated protein 55 (RAP55) localizes to mRNA processing bodies and stress granules. RNA *12*, 547–554.

Yang, Z., Jakymiw, A., Wood, M. R., Eystathioy, T., Rubin, R. L., Fritzler, M. J., and Chan, E. K. (2004). GW182 is critical for the stability of GW bodies expressed during the cell cycle and cell proliferation. J. Cell Sci. *117*, 5567–5578.

Zheng, D., Ezzeddine, N., Chen, C.Y., Zhu, W., He, X., and Shyu, A. B. (2008). Deadenylation is prerequisite for P-body formation and mRNA decay in mammalian cells. J. Cell Biol. *182*, 89–101.